

REPORT DOCUMENTATION PAGE

Form Approved
OMB No. 0704-0188

Public reporting burden for this collection of information is estimated to average 1 hour per response, including the time for reviewing instructions, searching existing data sources, gathering and maintaining the data needed, and completing and reviewing this collection of information. Send comments regarding this burden estimate or any other aspect of this collection of information, including suggestions for reducing this burden to Department of Defense, Washington Headquarters Services, Directorate for Information Operations and Reports (0704-0188), 1215 Jefferson Davis Highway, Suite 1204, Arlington, VA 22202-4302. Respondents should be aware that notwithstanding any other provision of law, no person shall be subject to any penalty for failing to comply with a collection of information if it does not display a currently valid OMB control number. PLEASE DO NOT RETURN YOUR FORM TO THE ABOVE ADDRESS.

1. REPORT DATE (DD-MM-YYYY)

2. REPORT TYPE

Technical Paper

3. DATES COVERED (From - To)

4. TITLE AND SUBTITLE

5a. CONTRACT NUMBER

5b. GRANT NUMBER

5c. PROGRAM ELEMENT NUMBER

62500F

6. AUTHOR(S)

5d. PROJECT NUMBER

2308

5e. TASK NUMBER

M4S7

5f. WORK UNIT NUMBER

345382

7. PERFORMING ORGANIZATION NAME(S) AND ADDRESS(ES)

8. PERFORMING ORGANIZATION
REPORT

9. SPONSORING / MONITORING AGENCY NAME(S) AND ADDRESS(ES)

Air Force Research Laboratory (AFMC)
AFRL/PRS
5 Pollux Drive.
Edwards AFB CA 93524-7048

10. SPONSOR/MONITOR'S
ACRONYM(S)

11. SPONSOR/MONITOR'S
NUMBER(S)

12. DISTRIBUTION / AVAILABILITY STATEMENT

Approved for public release; distribution unlimited.

13. SUPPLEMENTARY NOTES

See attached 13 papers, all with the information on this page.

14. ABSTRACT

15. SUBJECT TERMS

16. SECURITY CLASSIFICATION OF:

a. REPORT

Unclassified

b. ABSTRACT

Unclassified

c. THIS PAGE

Unclassified

17. LIMITATION
OF ABSTRACT

A

18. NUMBER
OF PAGES

19a. NAME OF RESPONSIBLE
PERSON

Kenette Gfeller

19b. TELEPHONE NUMBER

(include area code)
(661) 275-5016

Standard Form 298 (Rev. 8-98)
Prescribed by ANSI Std. Z39.18

Frequency-Domain Electromagnetic Characteristics of a 26-Kilowatt Ammonia Arcjet

L. K. Johnson, A. Rivera, M. Lundquist,
T. M. Sanks, A. Sutton, D. R. Bromaghim

Reprinted from

Journal of Spacecraft and Rockets

Volume 33, Number 1, Pages 137-143



A publication of the
American Institute of Aeronautics and Astronautics, Inc.
370 L'Enfant Promenade, SW
Washington, DC 20024-2518

Frequency-Domain Electromagnetic Characteristics of a 26-Kilowatt Ammonia Arcjet

L. K. Johnson,* A. Rivera,* and M. Lundquist*

The Aerospace Corporation, Los Angeles, California 90009

T. M. Sanks† and A. Sutton†

Phillips Laboratory, Edwards Air Force Base, California 93524-7190

and

D. R. Bromaghin‡

SPARTA, Inc., Edwards Air Force Base, California 93524-7190

Arcjet thrusters employ an arc discharge to heat propellant, which expands through a nozzle to produce thrust. Spacecraft designers who desire to exploit the enhanced specific impulse of arcjets have expressed concern about the electromagnetic environment produced by the thrusters. Laboratory tests were performed to investigate the electromagnetic environment produced by a 26-kW ammonia arcjet in the frequency domain from dc to 10 GHz using antennas intended to characterize electric and magnetic fields. Results obtained with a 30-cm monopole antenna exposed to the arcjet plume correspond to those of similar ground tests at lower power. When the antenna was shielded from electrical contact with the plume by a Pyrex® cover, signal levels dropped sharply at all frequencies. With a covered 30-cm monopole antenna near the arcjet plume, arcjet-on signals exceeded ambient levels over the frequency range 10 kHz–5 MHz. The maximum signal level typically exceeded the ambient level of 40 dB μ V/MHz by approximately 27 dB μ V/MHz near 200 kHz. A likely explanation for the sharp reduction in signal level once the antenna electrode is covered is that electrons and ions from the plume are collected on the exposed antenna but not on the covered antenna. Signals on the shielded antenna may be interpreted as the result of propagating electric fields, but considerable uncertainty remains about the field source and the effects of the facility on the measurements. Although the electromagnetic fields produced by an arcjet operating as part of a satellite are probably lower than previously expected, these results raise new concerns about the character and spacecraft compatibility of the plasma from an arcjet plume.

Introduction

A WIDE range of electric propulsion systems is currently under development.¹ Low-power units (1–5 kW) are employed for stationkeeping, and medium- and high-power arcjet systems (5–30 kW) are being developed for on-orbit maneuvering and orbit transfer. Spacecraft engineers, with the responsibility to ensure the compatibility of spacecraft systems and payloads, have inquired about the electromagnetic interference (EMI) characteristics of arcjets. Electromagnetic signatures of low-power arcjets have been studied in detail by NASA² and TRW³ in ground tests, but no data exist for higher-power devices. This effort focuses on the characteristics of electromagnetic emissions from a 26-kW ammonia arcjet similar to that which will fly on the Electric Propulsion Space Experiment⁴ (ESEX).

ESEX constitutes one experiment among several to be launched aboard the Advanced Research and Global Observation Satellite (ARGOS).^{5,6} Instruments flown as part of ESEX will measure electromagnetic signatures from the arcjet over the range 1–12 GHz to prove compatibility with generic spacecraft transceivers. In support of the ARGOS and ESEX programs, ground tests were performed to assess the electromagnetic signatures of a 26-kW laboratory model arcjet.

Experimental Procedures

Two series of tests were performed. Facilities common to both included the vacuum equipment, arcjet, power supply, and cables external to the vacuum chamber; the measurement equipment and procedures differed considerably between the two test series.

The cylindrical, mild steel vacuum chamber in which the tests were conducted is 2.4 m in diameter and 3.7 m long.⁷ The chamber was evacuated through 46-cm lines approximately 21 m long, leading to several large pumping stations composed of Roots blowers and rotary pumps. At the nominal propellant flow rate of 240 mg/s, the chamber pressure was below 400 mtorr.

The test article was a laboratory model 26-kW ammonia arcjet (Fig. 1) similar to those first developed in the mid-1960s by NASA and the Air Force.⁸ Although structurally different from the ESEX flight unit, the test arcjet was constructed with the same materials and electrode geometry in the region of arc attachment and propellant expansion. The electrode gap is set by inserting the cathode until it contacts the anode, then withdrawing the cathode the specified distance, which for these tests is 6 mm. The arcjet nominally operates at 240-mg/s propellant feed rate and 100-V arc potential. The current drawn by the arcjet is 260 A at 26 kW and 150 A at 15 kW. The arcjet mounting fixture grounds the arcjet anode to the chamber, which is in turn connected to an earth ground. No significant differences are expected in ionization fraction, thrust, nozzle temperature and pressure, or other plume qualities between the test article and a flight-type arcjet. No sources of materials with low ionization potentials, which could lead to anomalously high ionization, were identified to be in contact with the propellant flow.

The arcjet was energized by a 750-A, 250-V dc Linde PC-601 power supply utilizing 480-V ac, three-phase primary power. The arcjet was connected to 4-0 welding cables 18 m long, which were twisted to minimize interference. An air-cooled, series ballast resistor ($\sim 0.1\Omega$) is used to monitor the arc current during routine operation. The vacuum chamber feedthrough for the electrical power was not coaxial. During the first series of tests, no specific measures were used to reduce interference from the power cables inside the vacuum chamber. The second series of tests employed first a twisted power cable, and later a custom-made coaxial cable. This latter cable was constructed by wrapping the conductors from one 4-0 cable around a second, insulated cable. The second series of tests also employed

Received Oct. 31, 1994; revision received May 25, 1995; accepted for publication July 11, 1995. This paper is declared a work of the U.S. Government and is not subject to copyright protection in the United States.

*Member, Technical Staff, M/S M5-754, P.O. Box 92957.

†Project Manager, OL-AC PL/RKCO.

‡Project Engineer.

20050815 027

a coaxial electrical connection between the arcjet body and power cable, as well as a steel cover for the power feedthrough to shield against interfering fields arising from the power-cable feedthrough loop area.

Propellant is supplied to the arcjet via a tube fitting modified to provide electrical isolation between the arcjet cathode and the propellant feed line, which is connected to chamber ground. During the interval between the two series of tests, the propellant feed system was modified, but delivered the same flow rate for both series.

Test Equipment and Procedure

In the first series of tests, a self-contained, computer-controlled EMI data acquisition system was used to collect the signals from antennas located within the vacuum chamber. This system was essentially automated. Using the antenna signal and user-input antenna calibration factors, the system performs the frequency scan and calculates a corresponding electric field. Voltages actually measured on the antennas were not typically retained in the data files. While such an automated system is appropriate for routine EMI qualification of manufactured devices, it provides little flexibility for experimental research. For example, posttest analyses to extract antenna voltages

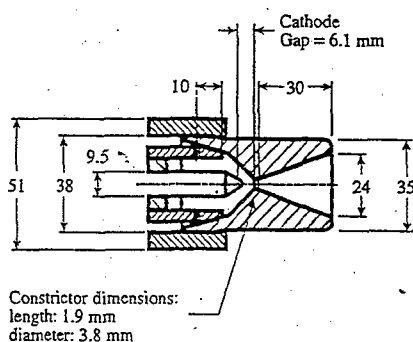


Fig. 1 Arcjet nozzle configuration. All dimensions are in millimeters.

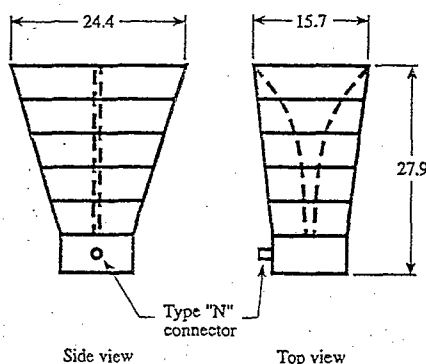


Fig. 2 Ridged-guide antenna. All dimensions are in centimeters.

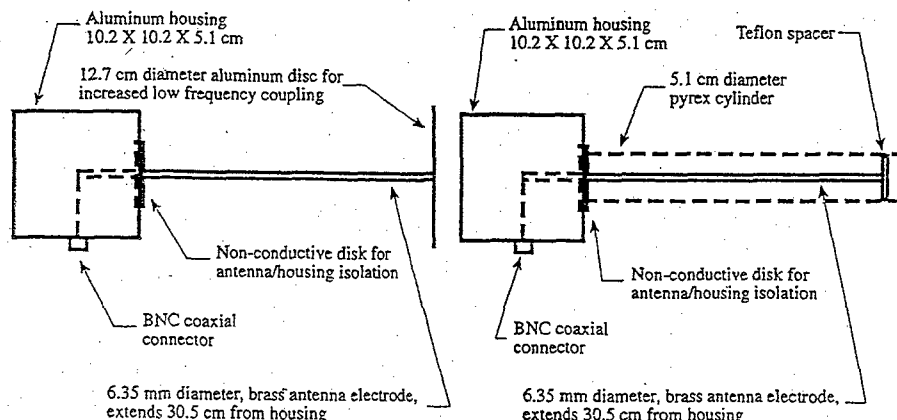


Fig. 3 End-loaded monopole antenna.

from electric field data required manual removal of the antenna factors, reversing the automated steps. The data acquisition system consisted of a small, calibrated ridged-guide horn antenna (1–10 GHz, Fig. 2), a network analyzer (1–10 GHz), and an EMI receiver (14 kHz–1 GHz). A custom made, end-loaded monopole antenna 30 cm long (Fig. 3) was used with the EMI receiver. This short antenna length was chosen to improve the reliability of electric field measurements by being significantly smaller than the facility and simulating the anticipated noise source. The insulating electrode support disk indicated in Fig. 3 was damaged in the first test series and replaced in the second series with Teflon[®], which suffered no damage. For the Pyrex[®]-covered monopole used in the second test series, a spacer was used to establish the minimum distance between the electrode and the outside of the cover at 22 mm.

A two-antenna procedure was employed to calibrate the monopole antennas. In this procedure, two identical antennas are installed in the vacuum chamber. The chamber door is closed, the pressure in the chamber is 1 atm, and the arcjet is off. One antenna is placed at the arcjet location and connected to a signal generator. The other antenna is located at its usual receive position and connected to the spectrum analyzer. At each calibration frequency, the coupling of the signal and receive antennas to the field is assumed to be the same, and thus the ratio of received to transmitted signal yields the square of the antenna coupling to the field. The coupling factor for frequencies other than calibration values is obtained by fitting a function of the form $a + bx^c$ to the antenna factors and interpolating. No rationale is required for such an interpolation function other than that it is smooth and monotonic. This calibration strategy, although robust and simple, does not allow for coupling or transmission changes caused by the plasma from an operating arcjet. Future experiments to examine changes in coupling during arcjet operation would be appropriate.

Figure 4 shows the arcjet and antenna arrangement in the vacuum chamber for both test series. The network analyzer and EMI receiver were located outside the vacuum chamber and connected to the antennas with an isolated-ground, coaxial vacuum feedthrough, which was used for both test series. Other antenna positions, such as on the arcjet centerline, proved impractical. Even in the positions used, the exposed polyethylene supports for the monopole antenna electrodes suffered heat-induced degradation, requiring the antennas to be refurbished several times during the first series of tests. High-frequency electromagnetic field absorbing material, identical to that used in anechoic EMI test facilities, was used in the first series of tests to reduce chamber effects from 1 to 10 GHz. An aluminum, open-ended liner (octagonal cross section, 3.6 m long and 1.8 m across, Fig. 4) was constructed to support 20 m² of absorber. Since it was anticipated that the performance of the absorber would degrade when subjected to the arcjet plume, testing at gigahertz frequencies was performed first. This absorber was damaged by the arcjet plume in the first test series and was not used in the second series.

In the second series of tests, the computer-controlled data acquisition system was replaced by a less automated system. Frequency-domain data were obtained by connecting antennas to a spectrum

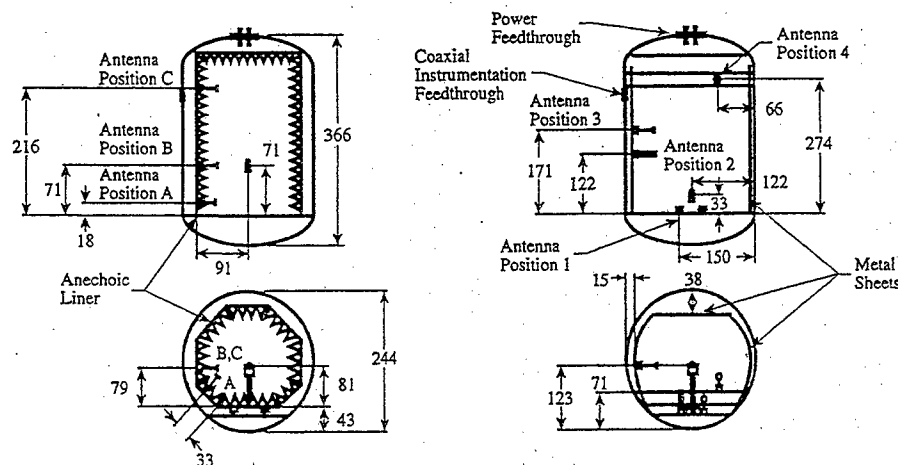


Fig. 4 Vacuum-chamber plan and antenna layout. All dimensions are in centimeters.

analyzer (50- Ω termination) interfaced to a computer. Spectrum-analyzer data so obtained corresponded to antenna signal voltages and constitutes the antenna response indicated in many of the figures presented here. Signal level data were converted into PC format for subsequent analysis. A current transformer was used to observe the time dependence of the arc current, and several different laboratory wave generators and amplifiers were used for antenna calibration. Antennas were located in the positions shown in Fig. 4. Sheet steel was used to protect the vacuum feedthroughs from the arcjet heat loads.

End-loaded monopole antennas similar to those in the first series of tests were used to obtain data from 10 Hz to 1 GHz. In an effort to reduce thruster-induced antenna damage, the polyethylene electrode supports of the monopole antennas were replaced with Teflon, and the all-thread electrodes were wrapped in aluminum foil. No antenna degradation was observed during the second series of tests. As testing progressed, additional antennas were fabricated to isolate the antenna electrode from charged particles in the arcjet plume. In this case, the end-loading discs were removed and 5-cm-diam Pyrex cylinders were used to cover the antenna electrodes (Fig. 3). These new antennas were recalibrated before use.

Magnetic fields associated with arcjet operation were measured using loop antennas. Ten wire turns of 0.01-m² area (0.1-m² total loop area) were employed from 10 Hz to 10 MHz (Fig. 5). To measure the horizontal component of the magnetic field, these antennas were mounted with the loop in a vertical plane and the loop normal parallel to the arcjet axis. Initially, the loop antenna housings were electrically common to the chamber. However, preliminary ambient measurements revealed large (50 dB μ V at 10-Hz bandwidth) signals at ac power-line frequencies, characteristic of ground loops between the antenna housings and the spectrum analyzer. When the housings were isolated from the chamber (and the electrical feedthrough grounds were isolated as well), the spurious signal was eliminated. The loop antenna housings were consequently isolated during all tests for which data are reported. In addition, the exposed metal surfaces of the loop shields (see Fig. 5) were covered with fiberglass adhesive tape. This procedure was carried out to prevent antenna overheating, but may also have functioned to prevent the ground side of the isolated loop antenna from collecting charge from the arcjet plasma. Loop antennas were calibrated using the two-antenna method. Although the vacuum chamber was not used for these calibrations, the antennas were arranged with the same relative location and orientation in another laboratory for the calibration. The calibration so obtained was verified using standard electromagnetic models.

In both series of tests, the arcjet was started by applying 440 V across the electrodes while flowing 230 mg/s of argon through the thruster, which resulted in arc initiation and subsequent continuous operation at 4 kW (150 A, 27 V). Once the arcjet reached thermal equilibrium with argon, ammonia was added to the propellant flow as the argon flow was slowly reduced to zero, increasing the power level to 15 kW (150 A, 100 V). After arcjet thermal equilibrium was

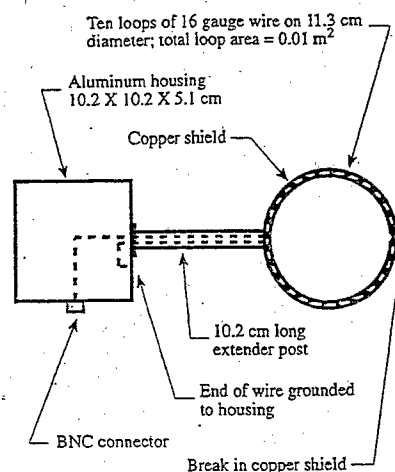


Fig. 5 Loop antennas used in second test series.

attained with ammonia as the propellant, the power-supply current was adjusted to perform tests at 15 and 26 kW.

Ambient measurements were made with the arcjet off and the chamber door closed for both series of tests. No significant differences were observed between ambient data collected under vacuum and at atmospheric pressure. Ambient measurements were also made outside the chamber and showed moderate signals at typical FM broadcast frequencies (~ 100 MHz). Comparing the ambient signals inside and outside the chamber, the shielding effect of the chamber was evident as a ~ 20 -dB reduction in observed broadcast signal levels.

In the second series of tests, frequency-domain data were acquired by setting the bandwidth and reference level on the spectrum analyzer and initiating a 1000-point sweep. Sweeps were taken over a preset frequency range (typically one decade, such as 0.1–1 MHz), and data from several such sweeps were assembled into a convenient format to cover a larger frequency range (e.g., 10 Hz–10 MHz). The data are presented using a logarithmic scale in the accompanying figures. Sweeps of different acquisition bandwidths were normalized to obtain a broadband response. In the logarithmic plots presented here, fluctuations in evenly sampled data points are compacted towards the high-frequency end of the sweep, giving a spurious impression of more noise.

Results and Discussion

During the second test series, the signal induced by the arcjet did not exhibit a regular waveform when observed on an oscilloscope, and so data from both series were analyzed considering the noise source to be uncorrelated. Thus, bandwidth correction factors of $10 \log(\text{signal})$ were applied to normalize observed signals. This amounts to an assertion of noise characterized by constant power

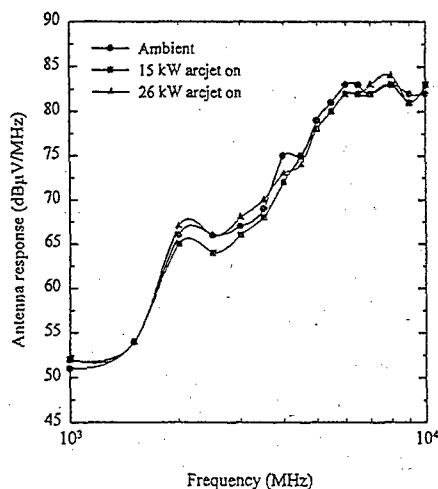


Fig. 6 Experimental results using ridged guide horn antenna.

per unit bandwidth. On the other hand, it is customary for EMI engineers to make the worst-case assumption that all noise signals are correlated, and EMI standards are typically presented in units consistent with correlated noise, i.e., V/Hz rather than $V/\sqrt{\text{Hz}}$. The data in this paper is presented in correlated-source units for utility and consistency.

Data obtained in these tests were repeatable to within ± 2.5 dB, and the calibration interpolation yields an uncertainty of 3 dB at each frequency, leading together to a combined uncertainty of approximately 4 dB for these measurements. However, uncertainties arising from the test environment's lack of fidelity to flight conditions easily overwhelm systematic uncertainties within the measurement setup. For this reason, no systematic-uncertainty analysis has been performed. Several factors have at least been identified that could undermine the fidelity of these data to flight results; and it is appropriate to list them here, unquantified. The significant sources of uncertainty include, in decreasing order of importance: 1) chamber pressure, 2) chamber electromagnetic effects (resonances, etc.), and 3) the nonflight-type power supply. Since each of these could cause order-of-magnitude changes in antenna response, it would be inappropriate to estimate an overall uncertainty, relative to flight expectations, for these measurements.

The particular relevance and utility of the data presented here involves the striking difference between spectra collected with uncovered and covered electrodes and the identification of this difference with the presence of the arcjet plasma. No characteristics of the test setup have been identified that would lead to an unusual plume ionization fraction in these ground tests. In flight, the arcjet is expected to produce a plasma similar to that observed here. Differences in plasma density would result primarily from less collisional plasma recombination in space. If anything, higher plasma density (and perhaps current collected by uncovered electrodes) would consequently be expected on an operating satellite.

First Test Series

Signals collected by the ridged-guide antenna over the frequency range 1–10 GHz are shown in Fig. 6; both ambient and arcjet-on sweeps are shown. No significant differences were observed between ambient and arcjet-on traces, and the observed increase in signal with frequency is indicative of the network analyzer's sensitivity rather than actual ambient fields. Signals obtained with the monopole antennas in positions B and C (see Fig. 4) over the frequency range 14 kHz–1 GHz are shown in Fig. 7. One ambient sweep as well as 15- and 26-kW arcjet-on sweeps are provided. The signals received at position A are similar to those from position C, and no signals of significance were observed above 100 MHz. The results from the ridged-guide and monopole antennas agree reasonably well at 1 GHz, where they can be compared, although again, the observed levels are an indication of instrument limitations rather than ambient fields.

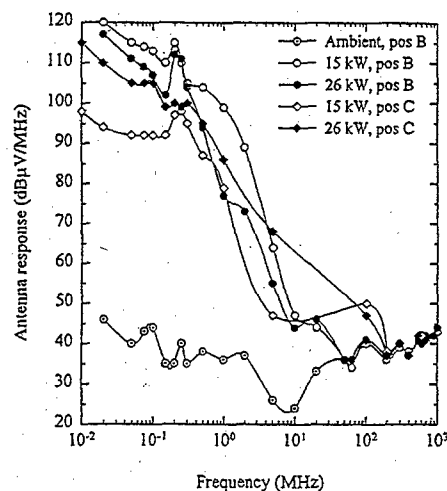


Fig. 7 Summary of experimental results using end-loaded monopole antenna in first test series.

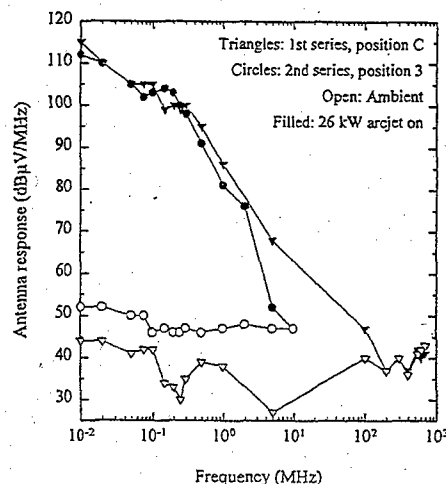


Fig. 8 Comparison between test series of 26-kW end-loaded monopole results.

Second Test Series

The principal objective of the second series of tests was to verify the results of the first series. Secondary objectives involved isolating the source of observed signals and using the loop antennas to assess arcjet-induced magnetic fields. Frequency-domain tests performed with uncovered end-loaded monopoles, shown in Fig. 8 along with results from the first test series, satisfied the principal objective. The second series of tests shows a higher ambient level, which is a result of spectrum-analyzer settings rather than differences in ambient fields. The two arcjet-on traces agree very well in the regions of overlap. The uncovered electrodes of the two test series have very similar geometries and clearly collect charge from the arcjet plasma in about the same way. Agreement is good except near 10 MHz, where the second-series results fall below the first series by 10–15 dB. No explanation has been developed for this difference.

The noncoaxial arcjet mount and cable were used for the second series of tests to reproduce the conditions of the first series. The second-series sweeps closely examined the frequency range below 10 MHz, where signals above ambient were appreciable. The data are accompanied by an indication of the acquisition bandwidth for each sweep. Boundaries between regions of differing acquisition bandwidth yield some indication of the signal's coherence characteristics. The continuity of the normalized results at these boundaries provides evidence that arcjet-induced signals were largely uncorrelated.

Initial efforts to isolate the source of observed signals involved installing the coaxial arcjet mount and cable. Subsequent frequency sweeps using the end-loaded monopoles revealed no significant ($< \pm 3$ dB) changes. The coaxial power feed system was used for

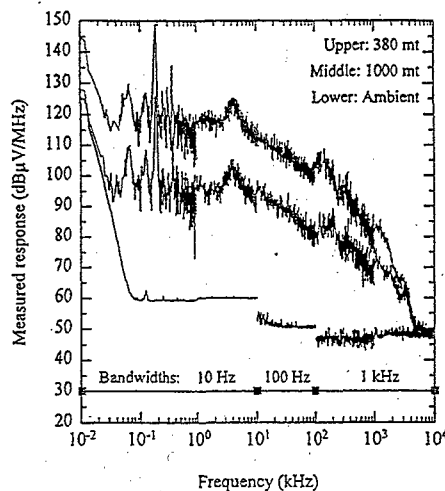


Fig. 9 Comparison of 26-kW end-loaded monopole data at 1000- and 380-mtorr chamber pressure.

the remainder of the tests. The housing of an end-loaded monopole antenna was then isolated from the chamber to investigate crosstalk between chamber and antenna or possible ground loops; but again, frequency sweeps showed no significant changes.

To determine whether observations were affected by pressure, the chamber pressure was increased to approximately 1 torr by valving off two of the three pumping stations. An end-loaded monopole antenna was used to obtain the frequency-domain data shown in Fig. 9 along with comparable data obtained at 380 mtorr. The data reveal a 10–20-dB reduction in antenna signal at the higher pressure. In addition, the arcjet plume was visibly more confined to the axis at 1 torr than at 380 mtorr. Arcjet plumes contain appreciable numbers of electrons and ions,⁹ and a few percent of the plume may be ionized.¹⁰ The increased collision frequency associated with higher chamber pressure would tend to recombine a plasma more efficiently, so that fewer electrons or ions would be present at the antenna locations. The smaller signals at higher pressure suggest the antennas might be collecting current from the plasma. Electrons or ions collected by the antennas would produce a signal that does not correspond to an electric field.

To assess the extent of current collection by the antennas, frequency sweeps with the Pyrex-covered antennas were performed in position 2, in front and to the side of the thruster, as shown in Fig. 10, which also includes uncovered-antenna results obtained at position 3. These data reveal a 20–60-dB signal reduction at all frequencies, where antenna signals rise appreciably above ambient levels, indicating that a large portion of the open-electrode antenna signal arises from current collection. Frequency sweeps with the covered-electrode antenna at position 1, behind the thruster, are shown in Fig. 11. All monopole-antenna data, with electrodes both covered and exposed, exhibit a feature near 200 kHz, whose origin is undetermined.

The results of loop antenna measurements conducted to characterize magnetic fields are provided in Fig. 12. Data from both loop antennas display features at approximately 200 kHz, and the loop antenna mounted behind the arcjet, 6 cm from the coaxial cable, displays a number of other features as well, including a broad peak at 10 kHz and several peaks over the range 1–10 MHz. The coaxial cable was not expected to suppress magnetic fields generated by current ripple as effectively as it suppressed electric fields. Consequently, features in the loop-antenna data located near the cable are probably due to power-line current ripple.

It is appropriate to briefly compare the operating conditions of these ground tests with those of an electric-propulsion thruster installed on a satellite. The power processor for a spacecraft-mounted arcjet is likely to employ switching regulation, whereas the welding power supply used for these tests does not. The ac characteristics of the two supplies can be expected to be quite different, which may have an effect on the high-frequency noise produced. A current probe mounted on the arcjet power lead from the welding supply, which operates on three-phase ac power, not surprisingly shows

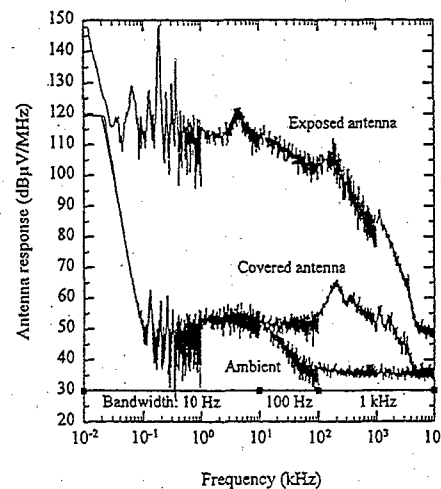


Fig. 10 Antenna response of Pyrex-covered monopole antenna positioned in front and to the side of thruster (see Fig. 4).

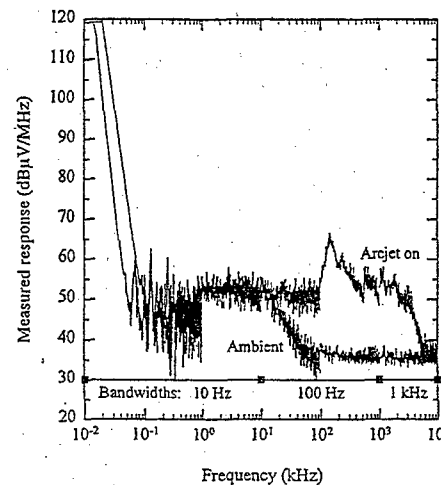


Fig. 11 Antenna response of Pyrex-covered monopole antenna behind thruster (see Fig. 4).

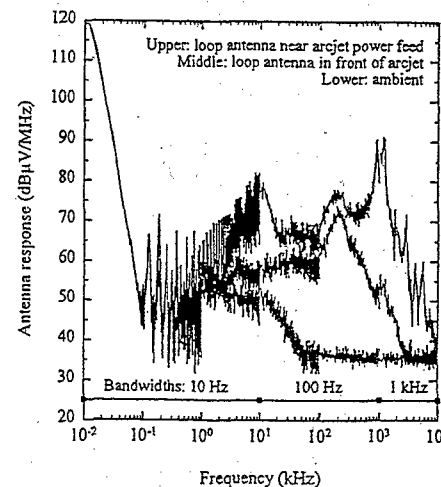


Fig. 12 Antenna response of magnetic field antennas.

a 180-Hz periodicity. This frequency, along with lower and higher harmonics, is evident in Fig. 9 and throughout the frequency sweeps of the second test series, and it is reasonable to conclude that these features are a signature of the power supply. A spacecraft power processor, switching at 10–25 kHz, can be expected to produce a large series of features associated with the switching frequency. The current-probe waveform revealed a nonsinusoidal current ripple of approximately 88 A peak to peak, or 31 A rms, over the 180-Hz waveform on the welding power supply. Typical current ripple^{11,12}

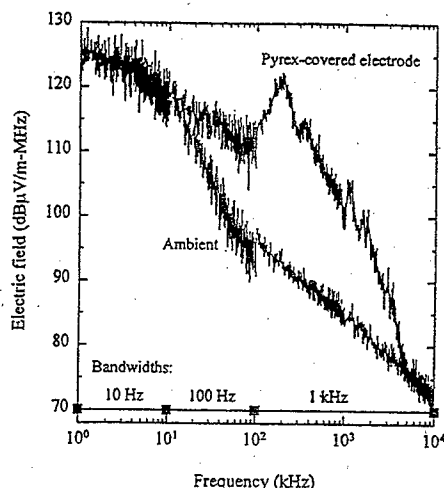


Fig. 13 Electric fields obtained with covered monopole antennas.

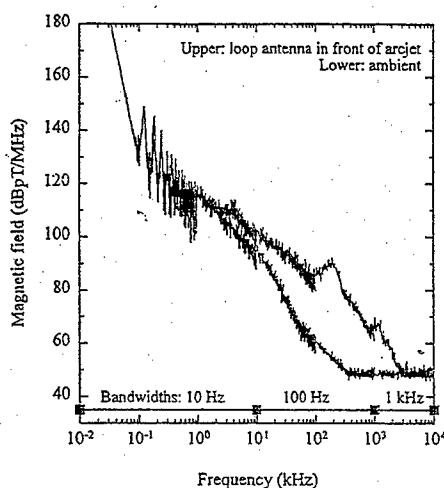


Fig. 14 Magnetic fields determined by loop antenna.

from an arcjet power processing unit is 10–20% at the 10–25-kHz switching frequency. This slow and relatively large oscillation in arcjet operating conditions, therefore, was not a good simulation of a spacecraft power processor. Although the characteristics of the power supply have an influence on the plasma properties of the arcjet plume (by affecting the electron temperature and density and excited-species populations¹¹), such differences are likely to be significantly smaller than the differences observed in the present tests between uncovered and covered antennas.

Another difference between this ground test and a spacecraft installation is the degree of vacuum into which the arcjet plume expands. These ground tests were conducted at a background pressure between 5 and 6 orders of magnitude higher than that of a satellite orbit. If the arcjet could simply be regarded as a well-characterized source of electromagnetic fields, this difference might be immaterial. Unfortunately, these and other tests^{9,10} indicate that the arcjet is the source of a plasma with a substantial charge density. The plasma density and propagation of fields through a plasma are governed in part by the number of charge-recombining collisions occurring, which in turn is determined by, among other quantities, the neutral-particle number density. Thus, a satisfactory simulation of the arcjet-induced environment, both for plasma contact effects (such as those measured by the uncovered monopole antenna) and for electromagnetic field effects (measured by the Pyrex-covered antenna), requires a better vacuum capability than those used in these tests.

It may be appropriate to relate the signals gathered from the glass-covered monopole and loop antennas to electromagnetic fields. The two-antenna calibration technique employed rests on two assumptions, namely, that conditions that could influence the propagation

of fields remain unchanged between calibration and test, and that the antenna geometry is a reasonable simulation of the field source. Unfortunately, the plasma produced by the arcjet could be the effective source of fields or could substantially modify the propagation of fields. Nevertheless, it was felt that the data, transformed into field levels (Figs. 13 and 14), should at least be provided as a reference for future experimenters. Unfortunately, it is not appropriate to compare these electric field results with data from the TRW 1.4-kW arcjet EMI test,³ since the TRW antennas were not shielded from the plasma.

Conclusions

Measurements utilizing electrodes in contact with a plasma induced by an electric propulsion device reflect the character of the plasma rather than an electromagnetic field. It is more appropriate to regard such an electrode as an unbiased Langmuir probe than as an antenna. When a glass cover is placed over the electrode to shield it from charged particles, the measured signals dropped by 20–60 dB. Signals collected on a covered antenna with the arcjet in operation exceed ambient levels over the frequency range 10 kHz–5 MHz. Typically, for a covered 30-cm monopole antenna near the arcjet plume, the maximum signal exceeds the ambient level of 40 dBμV/MHz by approximately 27 dBμV/MHz near 200 kHz. These tests also determined that magnetic fields from the arcjet power cable contribute significantly to measured magnetic fields. The signals collected strongly reflect the ac characteristics of the power source.

In view of these observations, future testing should incorporate power-cable geometry and test power-supply characteristics closely matching those of flight units. EMI qualification tests for arcjet thruster systems should also utilize facilities that more accurately simulate flight conditions. Finally, these observations indicate that spacecraft integrators need to allow for electric-propulsion thruster plume plasmas in overall spacecraft designs.

Acknowledgments

These tests were conducted at the Electric Propulsion Laboratory at the Phillips Laboratory at Edwards Air Force Base, California. The arcjet design used for the tests was the result of a performance improvement program conducted by the Olin Aerospace Company, formerly Rocket Research Company, under an Air Force Contract. In the first test series, the data acquisition system was leased from Electro-Metrics, Inc. For the second series of tests, equipment included an HP 8566B spectrum analyzer, HP 9000 computer, and T&M Research Products current transformer. This work was supported by the ARGOS and ESEX program offices and the Aerospace Sponsored Research program. Tests were carried out with the assistance of Jon Helt of SMC/CU, Deborah Cirilo-Parker from The Aerospace Corporation, and Dennis Tilley from Phillips Laboratory; and useful discussions were held with Mark Dunbar from The Aerospace Corporation. The authors would like to thank Jim Bartley, Grant Caton, and Chris Kasten (of the Computer Science Corporation), as well as Jim Zimmerman of the Bennefield Anechoic Facility at Edwards Air Force Base, for technical support; and also thank Bill Wales at Aerospace for antenna fabrication.

References

- ¹Pollard, J. E., Jackson, D. E., Marvin, D. C., Jenkin, A. B., and Janson, S. W., "Electric Propulsion Flight Experience and Technology Readiness," AIAA Paper 93-2221, June 1993.
- ²Pencil, E. J., Sarmiento, C. J., Lichtin, D. A., Palchefskey, J. W., and Bogorad, A. L., "Low Power Arcjet System Spacecraft Impacts," AIAA Paper 93-2392, June 1993.
- ³Zafran, S., "Hydrazine Arcjet Propulsion System Integration Testing," International Electric Propulsion Conf., Paper 91-013, Oct. 1991.
- ⁴Biess, J. J., and Sutton, A. M., "Integration and Verification of a 30 kW Arcjet Spacecraft System," AIAA Paper 94-3143, June 1994.
- ⁵Turner, B. J., and Agardy, F. J., "The Advanced Research and Global Observation (ARGOS) Program," AIAA Paper 94-4580, Sept. 1994.
- ⁶Agardy, F. J., and Cleave, R. R., "A Strategy for Maximizing the Scientific Return Using a Multi-phased Mission Design for ARGOS," American Astronomical Society, Paper 93-594, Aug. 1993.

⁷Castillo, S., Andrews, J. C., and Sutton, A., "Dedicated Electric Propulsion Laboratory," AIAA Paper 90-2658, 1990; Sutton, A. M., and Castillo, S., "Arcjet Thruster Experimental Facility at the United States Air Force Phillips Laboratory," International Astronautical Federation, IAF-92-0617, Dec. 1992.

⁸Lichon, P. G., and Cassady, R. J., "Performance Improvement of 26 kW Ammonia Arcjet," AIAA Paper 90-2532, July 1990.

⁹Sovèy, S. S., Carney, L. M., and Knowles, S. C., "Electromagnetic Emission Experiences Using Electric Propulsion Systems," *Journal of Propulsion and Power*, Vol. 5, No. 5, 1989, pp. 534-547.

¹⁰Hoskins, W. A., Kull, A. E., and Butler, G. W., "Measurement of

Population and Temperature Profiles in an Arcjet Plume," AIAA Paper 92-3240, July 1992.

¹¹Spores, R. A., Pobst, J. A., Schilling, J. H., and Erwin, D. A., "Performance Effects of Interaction Between a Low-Power Arcjet and Its Power Processing Unit," AIAA Paper 92-3238, July 1992.

¹²Vaughan, C. E., Cassady, R. J., and Fisher, J. R., "Design Fabrication and Test of a 26 kW Arcjet and Power Conditioning Unit," International Electric Propulsion Conf., Paper 93-048, Sept. 1993.

T. C. Lin
Associate Editor